Design of a sub 100-femtosecond X-ray streak camera

Bin Li, P. P. Rajeev, B. Dobson, M. M. Notley and D. Neely
Central Laser Facility, STFC, Rutherford Appleton Laboratory, HSIC, Didcot, Oxon OX11 0QX, UK

G. Gregori, A. Cavalleri, P. Lau and J. Lynn
Department of Physics, University of Oxford, Oxford, OX1 3PU, UK

M. Benetou
University College of London, WC1 6BT, UK

L. Pickworth
Department of Physics, Blackett Laboratory, Imperial College London, London, SW7 2AZ, UK

F. H. Read
School of Physics and Astronomy, University of Manchester, Manchester M13 9PL, UK

P. Jaanimagi
Laboratory for Laser Energetics, University of Rochester, 250 East River Road, Rochester, NY 14623, USA

Contact | **bin.li@stfc.ac.uk**

Introduction

Streak cameras are ideally the best instruments to directly investigate transient and ultrafast phenomena, which occur in laser-matter interaction experiments, where the duration of the optical or X-ray emission (~100 fs or less) is comparable with the timescale for the structural arrangement of the ionic lattice [1]. Thus, the basic idea of time resolved diagnostics is of enormous appeal for the progress and understanding of non-equilibrium and ultrafast structural phase transitions [1]. This is particularly relevant in view of new facilities (such as free electron lasers and high harmonic sources), which are being commissioned and will provide high photon fluxes at the femtosecond timescale. In the 1990s conventional streak camera technology has been pushed to the 500 fs level, [2,3] but at the expense of any reasonable dynamic range, thus limiting its applicability to selected applications. Still, such temporal resolution is very far from the ultimate limit of 100 fs, which has been predicted for high-speed imaging based on streak camera technology [4].

Here, we present a state-of-art design of a novel streak tube concept able to achieve the breakthrough 100 fs time resolution without the drawbacks of conventional streak camera technology. This work concentrates on the analytical description of the principle and it is based on the numerical simulations performed by Jaanimagi [5], where this idea was originally first presented. The engineering design along with the preliminary stage of fabrication and calibration procedures is presented as well.

Many factors contribute to the time resolution limit in streak cameras based on electron focusing optics. The most important ones are the limit t due to the upswept image of the input slit, the electron transit time dispersion t_d (even if electrons are emitted at the same time at the photocathode, differences in their initial energy make the faster electron to arrive at the recording device earlier than the slower ones) and the space charge broadening, t_{sp} of the electron bunch due to Coulomb repulsions. While the static image contribution to the time resolution can be easily controlled by using a narrow input slit and high spatial resolution phosphors on the back of the deflecting plates, the other two effects are much more difficult to minimize. It can be shown, however, that in many relevant applications transit time dispersion is the most important limiting factor in determining the ultimate time resolution of the streak camera [5].

As discussed by Jaanimagi [5], compensation of the transit time dispersion can be achieved with a symmetric double cylindrical deflector analyzer (DCDA), as shown in figure 1. This configuration (which we will refer as 'S-optics') is in some respect one of the simplest electron optics to compensate for the flight time dispersion, since it only uses electrostatic fields. Typically, the electrons with kinetic energy E_k and energy distribution ε can be selected and confined to the near median ray trajectories within a DCDA, where the potential of inner cylinder V_1 is higher than that of the outer cylinder V_2, and satisfies,

$$E_{k0} = \frac{e \cdot (V_1 - V_2)}{\ln \frac{R_2}{R_1}} \qquad (1)$$

Non-relativistically, electrons will travel through the concentrically cylindrical tube and arrive at the first

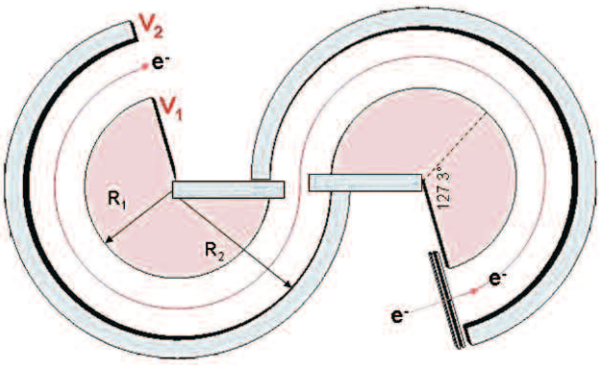

Figure 1. The 'S-optic', comprising of a slot photocathode electron accelerator and Double Cylindrical Deflector Analyzers in-series.

focusing node at the angle of rotaion ~127.3°, then the second node at the angle 254.6°, etc. Therefore the conceptual design of 'S-optics' as illustrated in figure 1 includes the rotation of anticlockwise for 254.6°, and then the clockwise for 254.6° sequentially.

However, a complete study of this streak camera design must also include the contribution of from the accelerating field at the photocathode. In this device the electrons emitted from the photocathode are accelerated but acquire positive, dispersion, meaning that higher energy electrons arrive earlier at the end of the accelerating section than slower electrons. The DCDA is then used to introduce a negative dispersion and compensate for the positive negative dispersion generated during acceleration.

Here, our effort is to investigate the feasibility and limit of applicability of such 'S-optic' configuration using simple analytical modeling, which is then validated with more sophisticated numerical calculations.

Analytical investigation

Diode

The 'S-optics' comprises a photocathode electron accelerator or a photodiode, attached to the entrance of the DCDA, to convert the optical or X-ray photon pulses into the electron pulses. The electron motion in the diode can be simply investigated using the idealized model of figure 2, where the cathode is assumed at ground (0 V) and the anode at the potential of 15 kV and separated by 20 mm. In a 1D geometry, the surfaces of the cathode and anode are assumed to be infinite, therefore any edge effect is negligible. For an electron starting at t=0 with null energy, the non-relativistic calculation yields,

$$t = \sqrt{\frac{2m_e s^2}{eV_0}} \tag{2}$$

Where t is the time of flight, m_e is the electron mass, s is the distance between the cathode and anode, and V_0 is the potential difference across the diode.

If we now consider an electron starting with energy ε, the non-relativistic electron flight time becomes,

$$t(\varepsilon) = \sqrt{\frac{2m_e s^2}{eV_0}} \cdot \sqrt{1+\frac{\varepsilon}{eV_0}} - \sqrt{\frac{2m_e s^2 \varepsilon}{eV_0^2}} \tag{3}$$

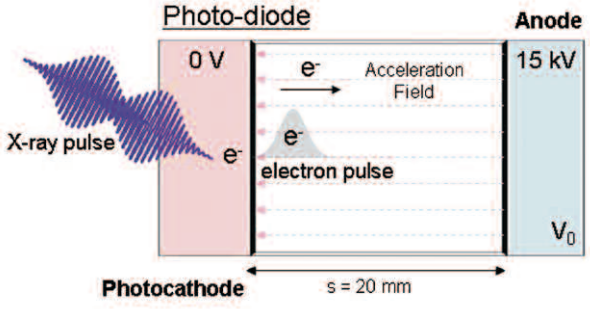

Figure 2. The electron motion in a photodiode.

When $\varepsilon << eV_0$, which is a typical case here (ε is at most a few eV), we have for the time dispersion,

$$\tau_1(\varepsilon) = t(\varepsilon) - t = -\sqrt{\frac{2m_e s^2 \varepsilon}{e^2 V_0^2}} + \sqrt{\frac{2m_e s^2}{eV_0}}\left(\frac{\varepsilon}{2eV_0}\right) \tag{4}$$

Using equation (4) we can easily calculate the difference of time of flight to cross the diode between an electron with initial energies of 1 eV, 10 eV or 100 eV and an electron with null starting energy. In Table 1, we compare our analytic results with numerical calculations either performed by Jaanimagi [5] or by the commercial package CST Particle Studio [6]. Both the numerical calculations include fully relativistic electrons (note that in Table 1, the negative sign indicates the positive dispersion).

Table 1. Flight time dispersion calculation in Diode.

ε-Energy difference (eV)	Equation 4 (ps)	CST-PS (ps)	Jaanimagi (ps)
1	-4.478	-4.473	-4.478
10	-14.035	-14.027	-14.031
100	-43.126	-43.087	-43.091

We notice that our analytic results compare very well with the numerical results for electrons with initial energies <10 eV. When the initial energy increases above ~100 eV, the relativistic effect becomes important, and the difference between our calculation and the two numerical results is larger than 30 fs.

Double cylindrical deflection analyzer

From the results discussed in the previous section, we see that energy differences as small as 0.0067% in the initial electron energy (1 eV compared to the final kinetic energy of 15 keV) would lead to ~4.5 ps dispersion at the end of a 20 mm travel distance. The double cylindrical deflection analyzer (DCDA) is implemented to compensate for this time dispersion.

The electron motion in DCDA can be described as [7],

$$m_e \frac{d^2R}{dt^2} = m_e \cdot R \cdot \omega^2 - eE(R) \tag{5}$$

Where the equation can be solved for electrons moving near the median ray $R = R_0 + \Delta R$ with energy distribution $E_k = E_{k0} + \varepsilon$, assuming angular momentum, $m_e R^2\omega$ conservation. In equation (5) $E(R)$ is the electric field at the radius R. The following initial conditions are applied, and E_{k0} is restricted by the condition given in equation (1).

$$\Delta R|_{t=0} = 0 \qquad \frac{d\Delta R}{dt}|_{t=0} = \sqrt{\frac{2E_{k0}}{m_e}} \cdot \sin\theta \tag{6}$$

(note t=0 corresponds to the time the electron start its travel in the DCDA). The solution of the electron radial motion is,

$$\Delta R(t) = \frac{\varepsilon R_0}{2E_{k0}} - \frac{\varepsilon R_0}{2E_{k0}}\cos(\sqrt{2}\omega_0 t) + \frac{\sqrt{2}R_0 \sin\theta}{4E_{k0}}[2E_{k0} + \varepsilon]\sin(\sqrt{2}\omega_0 t) \quad (7)$$

The electron with distribution ε will arrive at the intersection of the median ray, $\Delta R = 0$, when

$$t = \frac{2\pi n}{\sqrt{2}\omega_0} - \frac{2}{\sqrt{2}\omega_0}\tan^{-1}\left(\frac{\sqrt{2}\sin\theta}{2} + \frac{2\sqrt{2}E_{k0}\sin\theta}{\varepsilon}\right) \quad (8)$$

And in the limit of $\varepsilon << E_{k0}$ we get,

$$t = \frac{\pi(2n-1)}{\sqrt{2}\omega_0} + \frac{\varepsilon}{2E_{k0}\omega_0 \sin\theta} \quad (9)$$

The electron motion described by equation (9) is illustrated in figure 3, where electron entering into a DCDA with certain divergent angle will converge at its focal points per every ~127.3° Considering

$$\omega_0 = \left(\frac{2E_{k0}}{m_e}\right)^{1/2}\frac{1}{R_0}$$

and the average value of

$$\overline{\sin\theta} \sim 1/\sqrt{2\pi}$$

for Lambertian distribution, the dispersion generated by DCDA is given by,

$$\tau_2(\varepsilon) = \left(\frac{m_e}{E_{ko}}\right)^{1/2}\frac{\pi}{2E_{k0}}R_0\varepsilon \quad (10)$$

Differently from equation (4), this dispersion is negative (with positive sign, indicating that faster electrons arrive later than slower ones, since the travel path is longer for faster electrons) and this property can be utilized to compensate for the electron pulse dispersion generated by the diode acceleration at the photocathode. However, since the kinetic energy 15 keV is not anymore small compared to electron rest energy $m_e c^2 \approx 0.511 MeV$, relativistic effects must be taken into account,

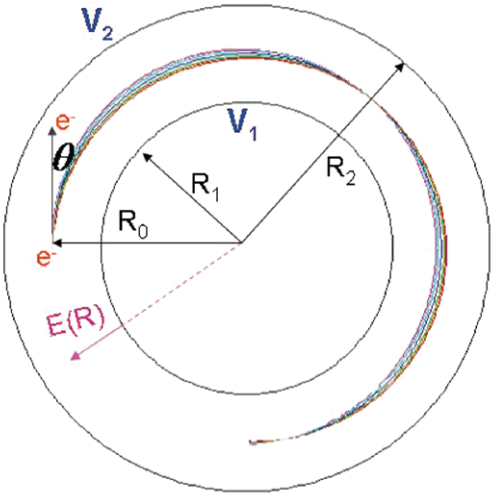

Figure 3. The electron motion in a typical concentric double cylindrical deflection analyzer.

$$eV_0 = \gamma \cdot E_{k0} = \frac{E_{k0}}{\sqrt{1 - E_{k0}/m_e c^2}}$$

In Table 2, we compared the results obtained from equation (10) and Jaanimagi[5] numerical calculations with R~206.88 mm >> s~20 mm, including the relativistic correction γ^{-1} ~0.9852. We notice very good agreement between the two calculations for various initial electron energies.

Table 2. Flight time dispersion calculation in DCDA.

ε-Energy difference from the median ray (eV)	Results from Eq.(10) (ps)	Jaanimagi (ps)
1	0.431	0.431
4	1.724	1.724
10	4.309	4.313
40	17.236	17.272

Combined system of photodiode and DCDA

From the previous discussion, the photoelectrons are initially accelerated to a potential V_0 in a short distance s, then travel in a DCDA near the median ray, so that the overall time spread in the combined system can be calculated as the sum of equation (4) and equation (10), where $E_{k0} = \gamma^{-1} eV_0$.

$$\approx -\left(\frac{2m_e s^2}{e^2 V_0^2}\right)^{1/2}\varepsilon^{1/2} + \left(\frac{m_e}{\gamma^{-1}eV_0}\right)^{1/2}\cdot\frac{\pi R}{2\gamma^{-1}eV_0}\varepsilon \quad (11)$$

According to equation (11), we can always choose a specific R, which is close to the median ray R_0, to minimize the overall time spread in diode and DCDA, meaning we are searching for the time difference $\tau(\varepsilon) \approx 0$. However any electron pulse has certain energy distribution at the most probable energy, so we are targeting to find the minimum time spread at a give electron probable energy distribution.

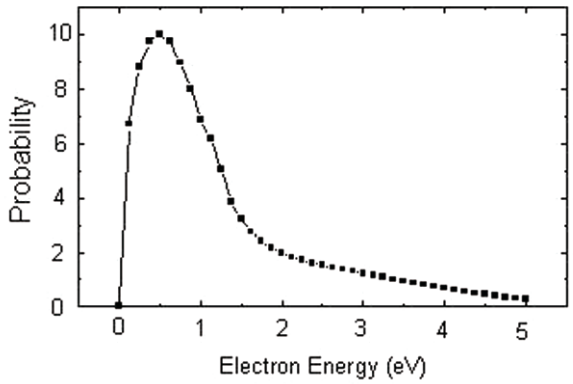

Figure 4. Initial energy distribution.

The most probable electron initial energy distribution from a typical photocathode, p(ε), is given by Jaanimagi[5] in figure 4. It has an asymmetric feature, peaks approximately at 0.5 eV, drops rapidly at the lower energy edge, falls down to 20% of the peak density at ~2 eV along with a long higher energy tails.

From equation (11), we have

$$\tau(\varepsilon) = -k_1 \cdot \varepsilon^{1/2} + k_2 \cdot R \cdot \varepsilon \quad (12)$$

At an acceleration field of 15kV/3mm, numerically we have $\tau = -0.00168492 \cdot \varepsilon^{1/2} + 1.30127 \times 10^7 \cdot R \cdot \varepsilon$ in SI unit, and for convenience, we can choose 1ps, 1mm and 1eV as the units of the time, distance and energy respectively, so the transition time is denoted as $\tau = -0.674426 \cdot \varepsilon^{1/2} + 0.00208486 \times 10^7 \cdot R \cdot \varepsilon$.

Again from equation (12), the minimum value is given by $\tau_{min} = -k_1^2/4Rk_2$ (= –0.238 ps), which is a negative value close to $\tau(\varepsilon) \approx 0$ and occurs when the condition

$$R = \frac{k_1}{2k_2\varepsilon}$$

(= 229 mm) is satisfied, this could be a simple method to find an optimal value for R approximately. More over, a given τ can be solved for a ε, and k_1 and k_2 are constants that only depend on the geometry of the systems (by equation (11)). The energy probability distribution function $p(\varepsilon)$ can be thus expressed as a function of τ, $p(\varepsilon^{-1}(\tau)) \Rightarrow f(t)$. We adopted a more generalized relation of τ and ε from Read[8],

$$\tau = [-k_1 + k_1' \sin^2\theta_1]\varepsilon^{1/2} + [k_2 - k_2' \sin^2\theta_2]R\varepsilon \quad (13),$$

where the angle θ_1 is emission angle (from the photocathode normal) of the ejected electrons and θ_2 refers to its projection in the non dispersive direction (i.e., with respect to the mid plane of the DCDA of figure 1). The constants k_1, k_2, k'_1, k'_2 are defined for a specific geometry of the problem. Assuming these given in terms of R, we can then evaluate the probability distribution functions $f(\tau)$ (data not shown), and find its FWHM $\Delta\tau$, as a function of R, as what is plotted in figure 5. It is clear that in order to compensate the time spread generated by the acceleration field of 15 kV in 3 mm, the compensator scale of R=250-300 mm would be the optimal values.

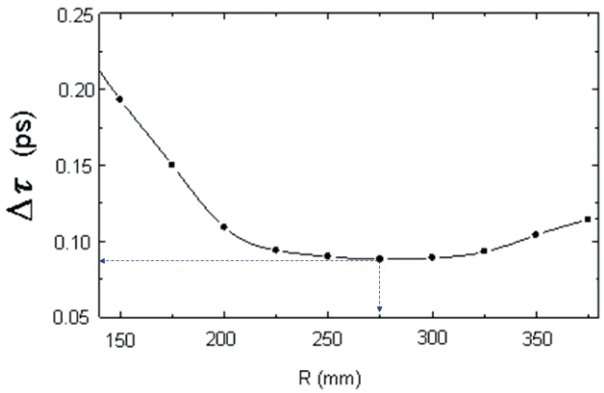

Figure 5. Dependence of the time spread $\Delta\tau$ on the DCDA compensator radius R.

Through the method we described in figure 5, we eventually obtain the optimal value of R, which is associated with the minimum time spread $\Delta\tau$ of the electron pulse. In figure 6, we plot the probability distribution at the optimum value of R=275 mm (for an acceleration field of 15 kV over 3 mm), and $\Delta\tau$ is ~90 fs, which indicates a breakthrough to <100 fs time resolution is achievable.

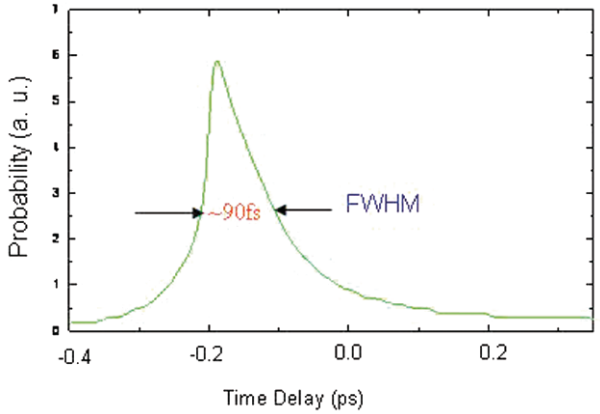

Figure 6. Probability distributions of the time delay τ for the value of optimal R=275mm that gives the minimum width $\Delta\tau$ ~90 fs.

Engineering design for the X-ray streak camera

Based on our analytic calculation and Jaanimagi's simulations, we have completed a full engineering of the novel 'S-optics' streak camera. The three dimensional view of this type of streak camera including two CDA in series to form the 'S-optics' shape is illustrated in figure 7.

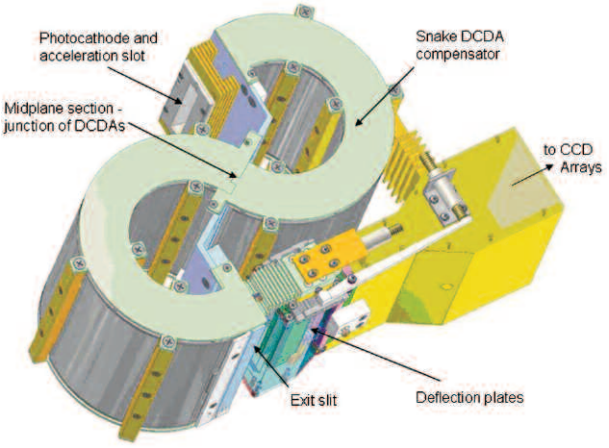

Figure 7. 3D view of 'S-optics' DCDA streak camera.

The photocathode along with the acceleration slot are anchored at the entrance of the compensator, where we nominal design for the acceleration field is set at V_0~5 kV over ~1 mm. (just below the break down field). The divergence of the electron beam and its position at the entrance of the DCDA is determined by a slit 50 μm slit, that can be adjusted to select the optimal compensator radius R~50 mm (from equation 11 or 12). Here, this value for the middle radius is smaller than our previously analytic results (229 mm) due to the different choice of the acceleration voltage and dimension at the photocathode.

The electron pulses are entering through the entrance slit, travelling through four focusing nodes in the 'S-optics', then passing through an exit slit with width of 10 μm into a deflection and focussing region which contains conventional streak camera optics and detection systems.

Discussion

Our analysis so far is mainly pertinent to single electron motion or non-interaction electron pulses. This is typically the case for low signal levels, when the photon number arriving at the photocathode is small, thus generating a small number of photoelectrons. However, when the signal increases in intensity, the interaction between the electrons could become important and essentially influence the motion and the time spread of the electron pulses, especially in the diode region, where the fields are strong and the electron current is confined in a small volume. The self interaction of the electrons among themselves is often referred to as 'space charge'. The electric potential in the diode is then given by Poisson's equation

$$\nabla^2 V(x) = -\frac{e \cdot n_e(x)}{\varepsilon_0},$$

where the cathode is assumed to freely emit electrons for a constant current flow crossing diode (1D approximation), with $V(x)$ and $n_e(x)$ the potential and electron density at x (0<x<s). Assuming that the electrons are emitted with null initial energy, we get [9]

$$t_{sp} = \frac{3}{2}\sqrt{\frac{2m_e s^2}{eV_0}} \tag{14}$$

and, when the initial energy is $\varepsilon = \frac{1}{2} m_e v_i^2$, the transient time changes as

$$t_{sp}(v_i) = \frac{3m_e s}{4eV_0}\left(\frac{2eV_0}{m_e}\right)^{\frac{1}{4}} \int_{v_i}^{\sqrt{\frac{2eV_0}{m_e}+v_i^2}} \frac{dv}{(v^2 - v_i^2)^{1/4}} \tag{15}$$

So the time dispersion for the space charge taken into account can be calculated from equation (14) and (15) numerically, which is different with the formula in equation (4) However, theoretically we can always adjust the DCDA compensator scale size R to minimize the overall time spread of the electron pulses. Thus, the equation (11) becomes to

$$\tau(\varepsilon) \approx -\frac{3}{2}\sqrt{\frac{2m_e s^2}{eV_0}} + \frac{3m_e s}{4eV_0}\left(\frac{2eV_0}{m_e}\right)^{\frac{1}{4}} \times \int_{\sqrt{\frac{2\varepsilon}{m_e}}}^{\sqrt{\frac{2(eV_0+\varepsilon)}{m_e}}} \frac{dv}{(v^2 - \frac{2\varepsilon}{m_e})^{1/4}} + \left(\frac{m_e}{\gamma^{-1} eV_0}\right)^{1/2} \cdot \frac{\pi R}{2\gamma^{-1} eV_0}\varepsilon \tag{16}$$

Implementation of the previously analytic conditions eV_0=15kV and s=3mm, leads to the optimal R=229mm and $\tau \approx -0.238$ps (from equation (11)); under the same conditions, we got $\tau \approx -7.7$ps from equation (16), which is obviously far from being compensated. However, applying the method we used to obtain the optimal R in non-space charge case will lead to a negative value. Then, we simple set $\tau \approx 0$, and get R=7.65m >> 229mm! Apparently, space charge could be one of the worst factors to resist improving the time-resolution of S-optics. Therefore we will need to avoid the photo-electron current in the extraction field much too high and maintain the 'S-optics' running below the breakdown condition to reduce the space charge effect.

Various commercial and private simulation programs include the treatment for space charge. MAFIA -an earlier particle tracking system to CST uses a particle in cell (PIC) method, which models the electron pulse as a cloud of charge spread over a number of meshing cells and solves Poisson's equation as the pulse progresses through the simulation [6]. However, the program doesn't work well the application discussed here, since a large number of mesh cells are required to achieve an ultimately sufficient short pulse (~500 fs), which causes extremely long computational times and large memory allocation.

B. Siwick approached to the space charge calculation using Molecular Dynamics in his PhD thesis [10]. He implemented a Barnes-Hut tree algorithm and a leapfrog integration scheme to solve the 'n electron' system. It could eventually be coupled with Jaanimagi's calculation to evaluate influence of the space charge in the 'S-optics'. More over, Qian and Elsayed-Ali applied a hydrodynamic model to derive the effect of space charge in a field free region analytically [11].

Here we proposed to design a novel steak camera that clearly has the potential to achieve 100-fs time resolution. It utilizes a combination of a modest extraction field at the photocathode and a double cylindrical deflection analyzer axial time-of-flight dispersion compensation with critical transverse energy selection. Currently, the detailed engineering drawing have been completed, and the Machine shop in University of Oxford is ready to start the machining and assembly. In the following year, our laboratory expects to perform the static focus test as well as the temporal compression calibration and performance, and ultimately we plan to deliver the first prototype of the snake streak camera within feasible future.

References

1. C. W. Siders *et al.*, *Science*, **286**, 1340 (1999).
2. A. J. Lieber *et al.*, *Electro-Opt. Syst. Des.*, **8**, 26 (1976).
3. M. M. Murnane *et al.*, *Appl. Phys. Lett.*, **56**, 1948 (1990).
4. E. K. Zavoisky and S. D. Fanchenko, *Appl. Optics*, **4**, 1155 (1965).
5. P. A. Jaanimagi, "Breaking the 100-fs barrier with a streak camera", *SPIE*, **5194**, 171 (2004).
6. CST, http://www.cst.com/Content/Products/PS/Overview.aspx
7. Klemperer & Barnett: *Electron Optics,* Third edition, Cambridge Monographs on physics, ch.10.4, pp.407-412.
8. F. Read, Private communication (March-July 2007).
9. J. R. Roth, *Industrial Plasma Engineering*, Vol 1, (IOP London, 1995).
10. B J Siwick, Dept. of Physics, University of Toronto, *PhD Thesis*, 2004.
11. B. L. Qian and H E Elsayed-Ali, *J. of Appl. Phys.*, **91**, 1, (2002).